Available online at www.sciencedirect.com
ScienceDirect
Journal of Power Sources 173 (2007) 478–486
JOURNAL OF POWER SOURCES
www.elsevier.com/locate/jpowsour

Immobilization of CO_2 by aqueous K_2CO_3 using microfibrous media entrapped small particulates for battery and fuel cell applications

Noppadon Sathitsuksanoh, Hongyun Yang, Donald R. Cahela, Bruce J. Tatarchuk [a,*]

[a] *Center of Microfibrous Materials Manufacturing, Department of Chemical Engineering, Auburn University, Auburn, AL 36849, United States*

Received 18 February 2007; received in revised form 18 April 2007; accepted 18 April 2007
Available online 4 May 2007

Abstract

This work focuses on developing a new adsorptive material and regenerable system for CO_2 sequestration to supply CO_2-free gas stream for low temperature and low carbon dioxide concentration applications, such as alkaline fuel cells, metal-air batteries, and portable air-purifying respirators. A novel microfibrous media has been introduced for carbon dioxide filtration from wet gas streams at room temperature. The use of microfibrous media in a composite bed maximizes the breakthrough capacity per unit volume and promotes high accessibility. The microfibrous media synergically combines the high contacting efficiency of the microfibrous matrix and the small internal mass transfer resistance of small particulates. The carbon dioxide adsorption capacity of the microfibrous media can be reversibly recovered. The incorporation of microfibrous media to the sodalime was observed. The result shows 120% improvement in the breakthrough capacity compared with the packed bed of the sodalime with the same volume. This approach can be applied to miniaturize the reactor and reduce thermal mass enhancing process intensification.

Keywords: Microfibrous media; Process intensification; Adsorption; Sequestration; Breakthrough

1. Introduction

Carbon dioxide sequestration has been of interest as the increment of CO_2 emissions contributes to the global warming and climate change [1]. Carbon dioxide is a product from many sources, such as human activities, vehicle emissions, and combustion in power plants. Some combustion applications release a large quantity of carbon dioxide, which needs to be removed prior to storage or being released into atmosphere such as coal gasification, fossil fuel power plants, and syngas production [2,3]. As a result, in recent years many carbon dioxide removal processes have been developed to meet the requirement of these applications as shown in Fig. 1 [4].

Fig. 1 shows a constructed diagram between the operational temperature of selected application and the range of carbon dioxide concentrations. There are a number of techniques that have been used to remove CO_2, such as Rectisol process (cold methanol), Selexol process (MEA), adsorption by solid sorbents, and absorption by liquid solvents. The use of liquid solvents is often employed in processes such as natural gas treating, gasification, and power plants. Such processes might be suitable for one application, but not another. Monoethanolaine (MEA) and hot postassium carbonate (K_2CO_3), for example, are often used in recovery of CO_2 in the ammonia industries, oil refineries, and petrochemical plants [5], both of which have high CO_2 removal capacity and efficiency. The same method cannot be applied for scrubbing CO_2 in fuel cells for portable electronic devices or in space cabin or submarines due to the large unit size and zero gravity limitation. An alternative, such as a use of solid sorbents and membrane processes has been of interest to overcome these disadvantages. The membrane processes are effective, but costly due to the high pressure required inside the membrane reactors to allow the gas or liquid to permeate through the membrane as well as the cleanliness of the gas. Small particulates can cause an undesired high pressure drop in the membrane reactor. In the case of solid sorbents, CaO is one of the most common carbon dioxide removal sorbents in power stations and coal gasification to enhance steam reforming. However, the reaction between CaO and CO_2 is a slow reaction at room temperature. As a result, CaO is usually operated at 500–600 °C. Molecular sieves often

* Corresponding author. Tel.: +1 334 844 2023; fax: +1 334 844 2065.
E-mail address: brucet@eng.auburn.edu (B.J. Tatarchuk).

0378-7753/$ – see front matter © 2007 Elsevier B.V. All rights reserved.
doi:10.1016/j.jpowsour.2007.04.047

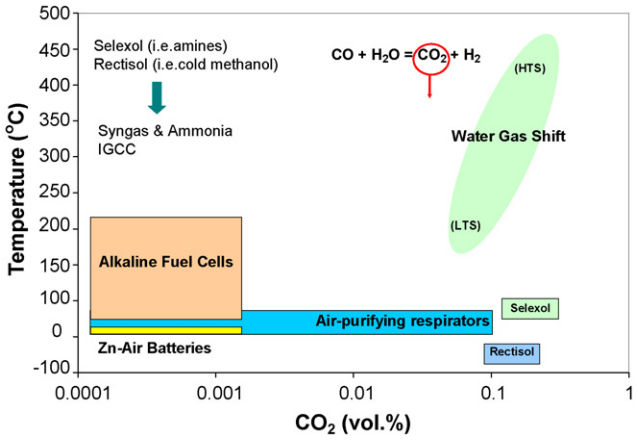

Fig. 1. CO_2 concentration levels in selected applications.

known as drying agents due to their moisture adsorption capacity by means of physical adsorption are often used to adsorb carbon dioxide in medical applications, such as during low-flow sevoflurane anaesthesia [6]. However, due to the high water adsorption, many beds of molecular sieves or silica are often incorporated in order to remove moisture prior to adsorption of carbon dioxide.

Alkaline fuel cells (AFCs) have been used since the mid-1960s by NASA in the Apollo and Space Shuttle Program due to their high efficiency of nearly 70% for generating electricity. However, high purity O_2 and H_2 are required to obtain high efficiency and extend the life of electrolyte (i.e. KOH) by preventing poisoning. As a result, AFCs are very costly; mainly due to the operational costs from frequent replacement of CO_2 scrubbers to maintain high purity H_2 and O_2. Zinc-air batteries, an example of metal-air batteries, are energized only when atmospheric oxygen is absorbed into the electrolyte through a gas-permeable, liquid-tight membrane. The electrolyte is typically potassium hydroxide utilizing OH^- as a charge carrier. Atmospheric oxygen is reduced at the cathode. The size of the air vent on the zinc-air batteries determines the power density of the cell. However, zinc-air batteries are very sensitive to temperature, moisture and carbon dioxide from air. The carbon dioxide from air usually leaks through the membrane forming carbonate compound, which reduces the OH^- in the electrolyte. The formation of this carbonate results in low conductivity and premature capacity reduction.

The objective of this study is to develop solutions for low concentration carbon dioxide applications. The use of aqueous solvents is not plausible for such applications as mentioned. This is not only because aqueous solvents are not amendable to random orientation, but also due to high operating cost, large unit size, low heat efficiency, solvent degradation, and equipment corrosion. Thus, the development of a new material for a cost-effective filtration with high CO_2 adsorption capacity is needed. The use of solid sorbents attracts much interest to overcome these disadvantages due to its low cost, low energy consumption, and wide range of operating temperatures and pressures. In current packed bed adsorbers, the use of small adsorbents results in high adsorption efficiency, but it is not practical due to high pressure drop or high energy consumption. The current effort is to utilize small particulates to reduce the intraparticle-limited mass transport and still maintain high adsorption efficiency and low pressure drop by means of microfibrous media by utilizing liquid potassium carbonate in packed bed operations for CO_2 removal under moist conditions. Microfibrous composite media [7–10] is used to entrap K_2CO_3(aq) as an "apparent solid" by incipient wetness impregnation. The adsorption of carbon dioxide results in the transformation of potassium carbonate into potassium hydrogen carbonate as shown in the following reaction:

$$K_2CO_3 + CO_2 + H_2O \Leftrightarrow 2KHCO_3 \quad (1)$$

The use of small particulates significantly enhances the intraparticle diffusion and allows high contacting efficiency. The nano-dispersed nature of K_2CO_3 combined with the use of small support particulates promotes high K_2CO_3 utilization, high contacting efficiency and high accessibility of K_2CO_3 while minimizing the pressure drop and lowering the heat of reaction.

2. Experimental

2.1. Adsorbent preparation

Supported K_2CO_3 sorbents were prepared using potassium carbonate sesquihydrate as a precursor, which is loaded onto the support by pseudo-incipient wetness impregnation. The potassium carbonate sesquihydrate was obtained from Alfa Aesar. Activated carbon was chosen as a support material due to its chemical inertness. Activated carbon particles were purchased from PICA-USA. The characteristics of the activated carbon particles are shown in Table 1.

Activated carbon particles were dried in the oven at 100 °C for 24 h prior to impregnation. The impregnation solution was prepared by adding potassium carbonate sesquihydrate and dionized water to obtain a desired concentration. The sorbents were then prepared by filling the pores of the porous supports at various loadings by varying the solution concentration to examine the effect of K_2CO_3 loading on CO_2 adsorption performance. After impregnation, the sorbents were then dried at 100 °C for 30 min. The volume of the sorbents was maintained at 10 cm^3; otherwise stated.

2.2. Preparation of microfibrous entrapped sorbents

A sintered metal microfibrous carrier was used to entrap 150–250 μm diameter support particulates by wet layer papermaking/sintering procedure. The composition of 6 in. preform media consists of 1 g of 8 μm nickel fibers, 3 g of 12 μm nickel

Table 1
Characteristics of activated carbon particles

Support	ACP
Size	150–250 μm, 1 mm
Density (g cm^{-3})	0.48
Pore volume (cm^3 g^{-1})	0.60
Manufacturer	PICA USA

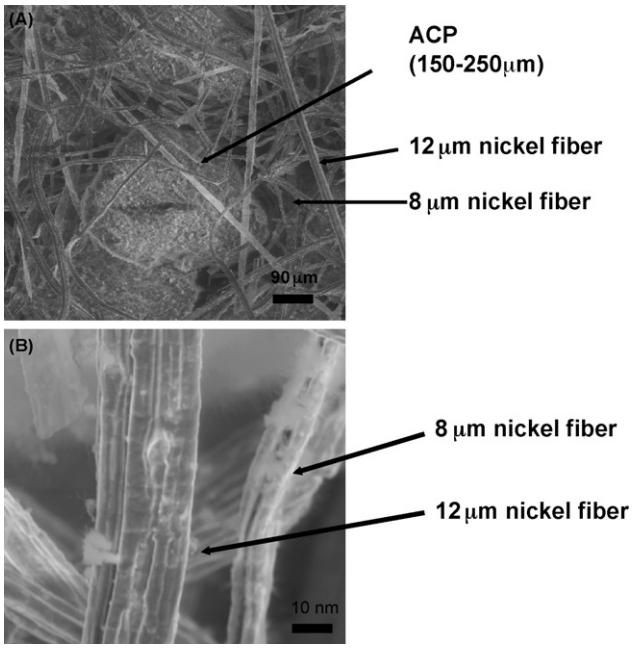

Fig. 2. Structure of microfibrous media; (A) microfibrous entrapped ACP; (B) microfibrous matrix.

fibers, 1 g of cellulose, and 10 g of activated carbon particles (15–250 μm).

One gram of 8 μm nickel fibers, 3 g of 12 μm nickel fibers, and 1 g of cellulose were added into water and stirred vigorously in a blender to produce a uniform suspension. The produced suspension and 10 g of 150–250 mm ACP were mixed in a 6 in. perform former under aeration. Six inches perform was then formed by filtration. The preform is then sintered in hydrogen atmosphere at 900 °C for 2 h. In this process, the cellulose in the preform is removed by gasification, and the nickel fibers microweld forming a sinter-locked matrix. The preform was then impregnated with impregnation solution. By utilizing the wet layer papermaking process, these particulates can be entrapped uniformly in the fibrous matrix as shown in the SEM micrograph in Fig. 2.

2.3. Breakthrough tests

The performance of adsorptive materials used for carbon dioxide removal was carried out at 20–30 °C in a packed-bed adsorber (1.5 cm i.d.) using simulated gas containing 1.5 vol.% and 2000 ppm CO_2 challenge concentration (C_0) in He as a test gas. The gas flux was then saturated with water vapor up to 2 vol.% (84% RH) prior to entering the reactor inlet at room temperature as shown in Fig. 3. The outlet CO_2 concentration was determined by CO_2 analyzer (PP Systems, USA). The CO_2 analyzer was calibrated against air and can detect CO_2 concentration as low as 1 ppm by utilizing Non-dispersive infra-red gas analysis. The downstream concentration (C) was recorded simultaneously at the sampling rate of 1 data point per second. The test results are expressed in term of variations of C/C_0 over time (breakthrough curves). The breakthrough concentration is defined at 50 ppm, unless otherwise stated.

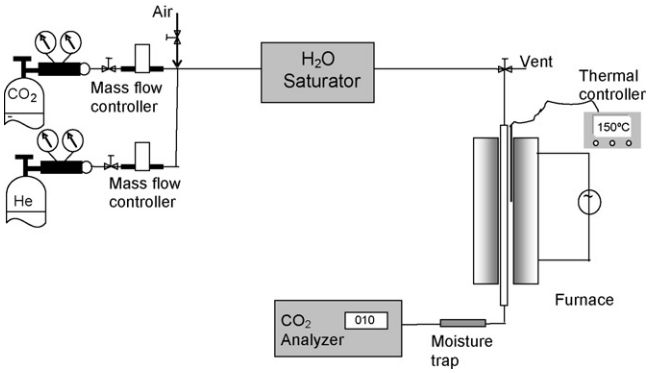

Fig. 3. Experimental apparatus.

The composite bed consists of a packed bed of sorbent particulates followed by a polishing sorbent layer as shown in Fig. 4. The influence of microfibrous media incorporating adsorption of solid sorbents on the breakthrough characteristics was studied.

A series of supported-K_2CO_3 sorbents were prepared in order to examine and compare the performance of a packed bed of K_2CO_3/ACP sorbents and a composite bed. A packed bed of Sodalime was then applied in a composite bed utilizing microfibrous media entrapped K_2CO_3/ACP sorbents as a polisher and performed breakthrough tests against the packed bed of Sodalime of the same volume for comparison.

Yoon and Nelson [11] have developed a model describing adsorption breakthrough curves on activated charcoal based on assumption that the rate of adsorption decreases as a function of adsorbate adsorption. This equation is simple and required no data on characteristics of the adsorbates and adsorbents. As a result, this model will be applied throughout this study. The Yoon and Nelson equation can be expressed as follows:

$$t = \tau + \frac{1}{k'} \ln \frac{C_b}{C_0 - C_b}$$

where k' is the rate constant (1 min^{-1}), τ the time corresponding to the saturation capacity(min), t the (sampling) breakthrough time (min), C_b the breakthrough (effluent) concentration of adsorbate (ppm), C_0 the initial inlet concentration of adsorbate (ppm). These values are determined from the experimental data by plotting $\ln[C_b/(C_0 - C_b)]$ versus time (t) according to Yoon and Nelson equation. If the accurate experimental data are

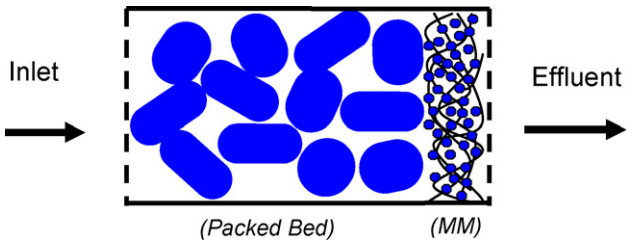

Fig. 4. Composite bed design.

obtained, this plot will result in a straight line with a slope of k' and the intercept of $-k'\tau$.

2.4. Sorbent characterization

The structural phase composition of the sorbents was then characterized by X-ray diffraction (XRD) using Cu Kα radiation from 20° to 60° with the scanning rate of 4° min^{-1}. Differential scanning calorimetry (DSC) was then used to determine the thermal stability of the sorbents at temperatures between 35 and 500 °C at the heating rate of 10 °C min^{-1} to determine the regeneration temperature. Scanning electron microscopy (SEM) was then employed to examine the robustness and structural integrity of the microfibrous media after cyclic adsorption/desorption.

3. Results and discussion

3.1. Effect of K_2CO_3 loadings

The ACP composite sorbents underwent breakthrough tests as shown in Fig. 5. It was found that an increase in K_2CO_3 loading yields an optimal point around 30 wt.%. The sorbent capacity reaches 0.01 g CO_2/total g of the sorbent, which is 30% utilization at room temperature. The ACP composite sorbents show sharp breakthrough curves indicative of high utilization of the sorbents.

The carbon dioxide adsorption capacity and K_2CO_3 utilization was calculated from the breakthrough data shown in Fig. 6. The CO_2 adsorption capacity of ACP-based sorbents can reach 0.012 g CO_2/total g of sorbents with utilization of 30%. This type of sorbent can be used in a large adsorber or in the processes that have many adsorbers as the saturated bed can undergo regeneration while using other adsorbers for adsorption. A highly porous material such as ACP is well suited for application in regeneration systems. The high porosity of ACP (0.48 g cm^{-3}) helps to disperse chemically active compound (K_2CO_3) in the pores, enhances the accessibility, and lowers regeneration temperatures.

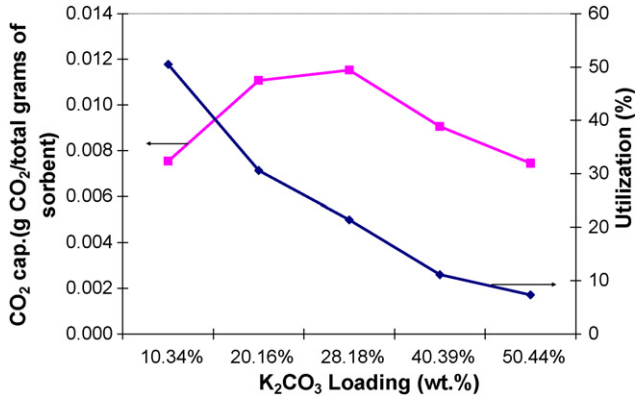

Fig. 6. CO_2 adsorption capacity and utilization of K_2CO_3/ACP sorbents at different K_2CO_3 loadings.

3.2. Effect of moisture contents on the CO_2 capacity of the sorbents

Based on Eq. (1), water is necessary as it appears as one of the reactants. It was found that additional water enhances the performance of the sorbents; however, it is not very well understood. In this section, three aspects of additional water are investigated: excess water (free water), crystallization water, and water from gas stream. A series of breakthrough experiments was conducted to understand the effect of water on carbon dioxide adsorption mechanism.

3.2.1. Effect of crystallization water

Fig. 7 shows breakthrough tests of 5 g of pure K_2CO_3 in dry and wet conditions. The breakthrough curve of the sorbent under dry condition shows no carbon dioxide adsorption capacity (residence time = 0.5 min). The challenge gas was then by-passed through a H_2O saturator prior to entering the adsorber and the breakthrough result shows an increase in carbon dioxide adsorption capacity compared to that of the dry condition.

The adsorption of carbon dioxide by potassium carbonate takes place in the surface layer of water formed by moisture carried by gas stream and the remaining water inside the sorbents. Carbon dioxide diffuses in the water layer and is neutralized by

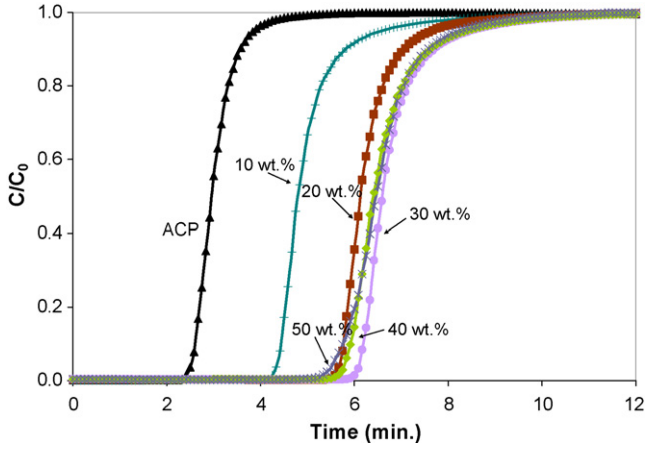

Fig. 5. Breakthrough curves of K_2CO_3/ACP at different K_2CO_3 loadings.

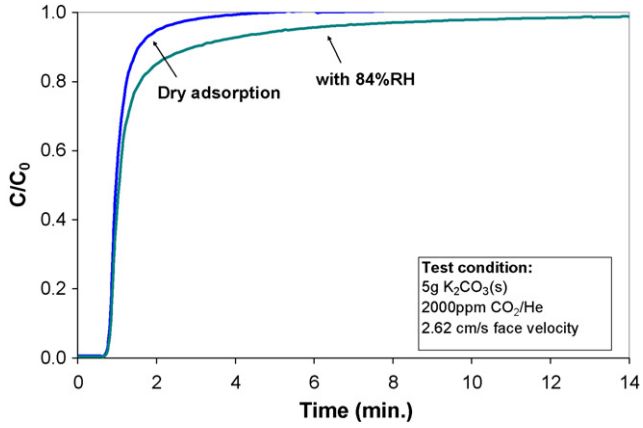

Fig. 7. Breakthrough curves of K_2CO_3 in dry and wet gas streams.

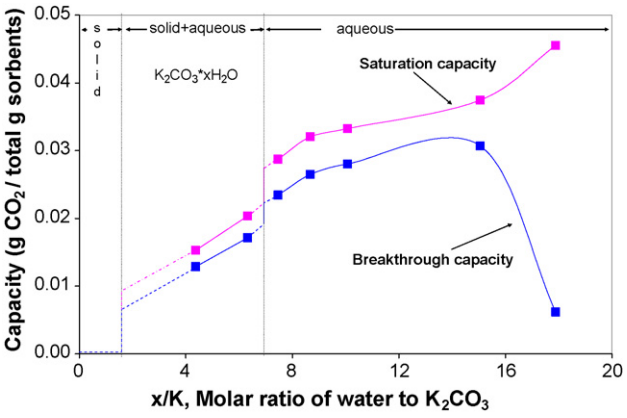

Fig. 8. CO_2 adsorption capacity at various moisture contents.

the dissolved K_2CO_3 as shown in the following reactions:

$$H_2O + CO_2 \Leftrightarrow H_2CO_3$$

$$H_2CO_3 \Leftrightarrow H^+ + HCO_3^-$$

$$HCO_3^- \Leftrightarrow H^+ + CO_3^{2-}$$

$$2H^+ + CO_3^{2-} + K_2CO_3 \Leftrightarrow 2KHCO_3$$

The solid K_2CO_3 sorbents do not adsorb carbon dioxide as shown in Fig. 7. An addition of water from the gas stream forms a water layer at the surface of the sorbents, but the hydration reaction is kinetically slow as shown in the late shift of the breakthrough curve ($C/C_0 \sim 0.5$). It is shown that insufficient crystallization water results in an additional step in order to hydrate the potassium carbonate. This is more likely a rate-determining step.

$$K_2CO_3 + xH_2O \rightarrow K_2CO_3{\cdot}xH_2O \quad (5)$$

3.2.2. Effect of remaining water during sorbent preparation

The prepared sorbents were dried in the oven at 100 °C at different drying times. The influence of drying time is to determine the remaining water in the sorbents. The ratio of water to potassium carbonate (x/K) inside the adsorbents is an important parameter. The maximum CO_2 adsorption capacity corresponds to the x/K ratio of 16 as shown in Fig. 8.

The x/K ratio indicates the state of the sorbents in the porous matrix. Based on the solubility and liquid density of K_2CO_3 as shown in Table 2, it is found that at x/K ratio of 1.5 and lower, the sorbents are in the solid state and yield low carbon dioxide adsorption capacity. As x/K ratio is increased between 1.5 and 7, a part of $K_2CO_3{\cdot}xH_2O$ dissolves in the additional water in the system and results in the mixture between

Table 2
Solubility and liquid density of K_2CO_3 and $KHCO_3$ at 25 °C

	Solubility (g solute/ 1000 g water)	Saturation density ($g\,cm^{-3}$)
K_2CO_3	1126	1.145
$KHCO_3$	333	1.165

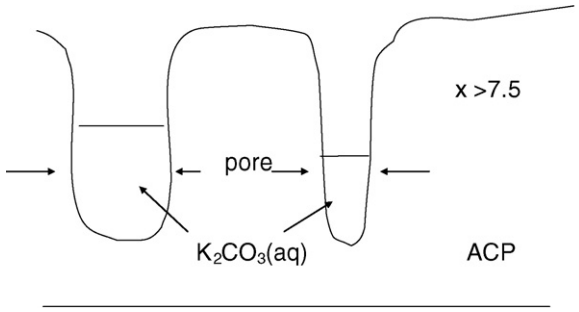

Fig. 9. Schematic phase diagram of K_2CO_3 in the pores of activated carbon.

solid and aqueous phase, which offers higher carbon dioxide adsorption capacity than those with lower x/K ratios. A further increase in x/K ratio higher than 7.5 causes all $K_2CO_3{\cdot}xH_2O$ to dissolve as evidenced by the solubility limit of K_2CO_3. At this state, the composite sorbents offer highest carbon dioxide adsorption capacity, which is preferably. Fig. 9 show the schematic of the composite sorbents in the ACP porous matrix.

The water layer formed on surface comes from remaining water in sorbents with different drying times. The phase of the sorbents is controlled by the solubility limit of K_2CO_3 and the amount of water remaining after drying. The composite sorbents need to create an aqueous environment (hydration) in order to adsorb carbon dioxide. If the aqueous environment is not created, then hydration is the rate-determining step. If an insufficient amount of water ($x/K < \text{or} = 1.5$) is available, the K_2CO_3 is in the form of solid, which needs to be dissolved in the water in the surface layer in order to capture carbon dioxide. An increase in the x/K ratios between 1.5 and 7 (additional water) causes K_2CO_3 to be partially dissolved in water (create aqueous environment) and results in a mixed phase between solid and aqueous. The K_2CO_3 in aqueous environment can readily react with carbon dioxide while the K_2CO_3(s) needs to create an aqueous environment by dissolving in the water surface, which results in higher carbon dioxide adsorption capacity than those with x/K ratio lower than 1.5. A further increase in x/K ratios beyond seven causes all K_2CO_3 to dissolve and readily react with carbon dioxide resulting in an increase in carbon dioxide adsorption capacity. At the highest x/K ratio, water completely fills the pores of the ACP, hindering adsorption of CO_2.

3.3. Effect of remaining water during adsorption

In the previous section, it was shown that additional water from the gas stream is required in order to maximize the formation of HCO_3^- to enhance the CO_2 adsorption capacity depending on the state of the composite sorbents. The sorbents in the aqueous form exhibit higher CO_2 adsorption capacity than those in solid or mixture between solid and liquid.

The K_2CO_3/ACP sorbents were tested under wet and dry conditions. The composite sorbents possess x/K ratio of 16 indicative of aqueous state, which readily adsorbs carbon dioxide. It is shown in Fig. 10 that additional water from gas stream improves

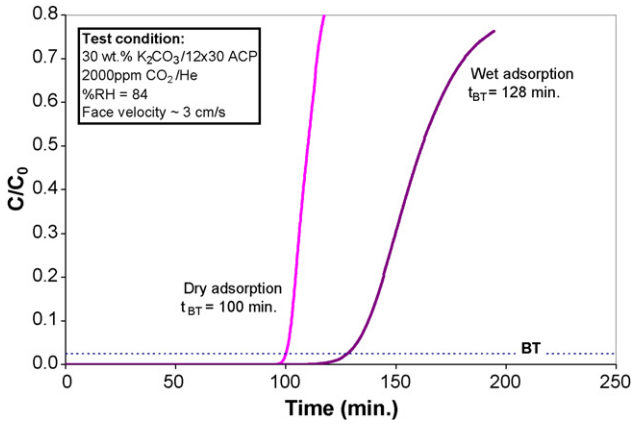

Fig. 10. Breakthrough curves of K_2CO_3/ACP in dry and wet gas streams.

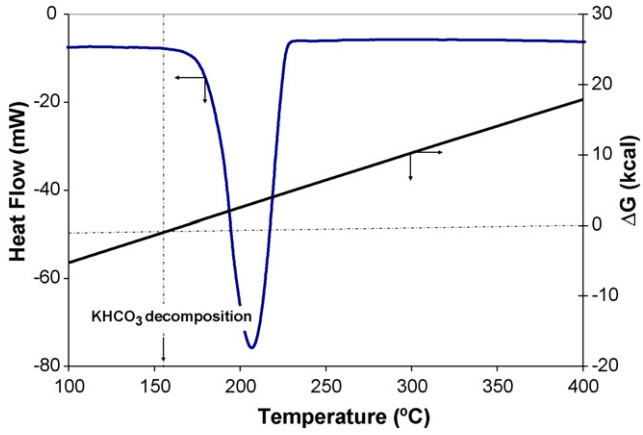

Fig. 11. DSC spectrum and calculated ΔG as a function of temperature.

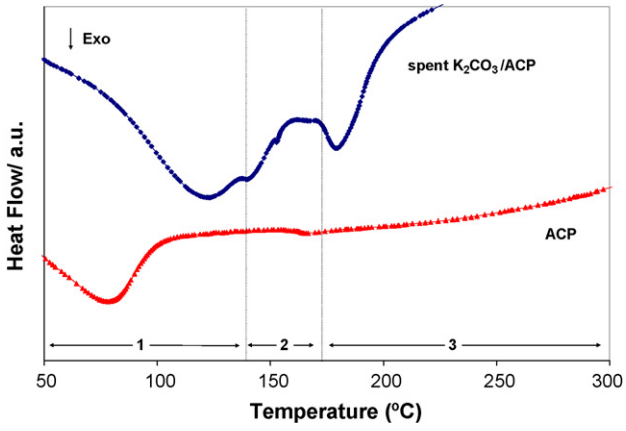

Fig. 12. DSC spectra of ACP and K_2CO_3 impregnated ACP.

breakthrough capacity by 28%. The state of the composite sorbents determines the rate of intermediate formation (HCO_3^-) in the surface layer (water layer). Since the water layer is already formed by water adsorption from the sorbent, additional water adsorption from the gas stream should not have any effect on the carbon dioxide adsorption capacity. In effect, additional water from gas stream might dilute the K_2CO_3(aq) in the composite sorbents and result in a drop in carbon dioxide adsorption capacity. However, an increase in breakthrough and saturation capacity of CO_2 was observed as seen in the shift of the breakthrough curve to the right side in Fig. 10. The high x/K ratio of the current composite sorbent indicates the amount of HCO_3^- formed in the surface layer and results in rapid formation of $KHCO_3$. Based on the difference in solubility and liquid density of K_2CO_3 and $KHCO_3$, precipitation of $KHCO_3$ is expected and the precipitation of $KHCO_3$ prevents utilization of the composite sorbents. As a result, the additional water adsorption from the gas stream is needed to stabilize the formation of $KHCO_3$ from precipitation, as seen in an increase in breakthrough time from 100 to 128 min.

3.4. Determination of regeneration temperature

DSC and thermodynamic calculation using HSC chemistry [12] were utilized to determine the decomposition of $KHCO_3$. The temperature where ΔG of formation has value of zero normally indicates the possibility of reverse reaction to take place. It is found that ΔG is zero around 167 °C indicative of decomposition of $KHCO_3$ forming K_2CO_3 as shown in Fig. 11.

The DSC experiment was conducted using bulk $KHCO_3$ with a heating rate of 10 °C min^{-1} from 35 to 500 °C. The DSC spectrum exhibits one exothermic peak with an onset around 150 °C, which confirms the possible decomposition of $KHCO_3$ at 150 °C.

The spent ACP composite sorbents were then tested by DSC. The result of the spent ACP composite sorbents shows three exothermic peaks as shown in Fig. 12. The first broad peak between 50 and 130 °C is associated with the evaporation of physically adsorbed water. The same broad peak was observed in the ACP particulate samples. The second peak between 130 and 169 °C was observed. This peak is associated with the dehydration of crystallization water. The third peak between 169 and 223 °C corresponds to the decomposition of $KHCO_3$. The spent composite sorbents were then regenerated at 150 °C and tested for carbon dioxide adsorption characteristics.

Fig. 13 shows the breakthrough curves of the freshly prepared composite sorbent and spent composite sorbents regenerated in

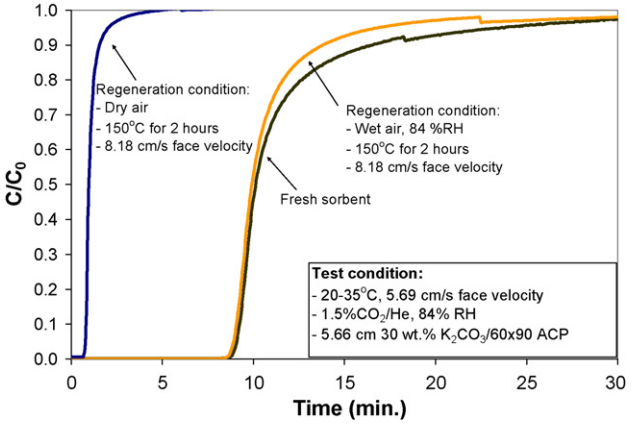

Fig. 13. Breakthrough curves of K_2CO_3/ACP in wet and dry regeneration conditions.

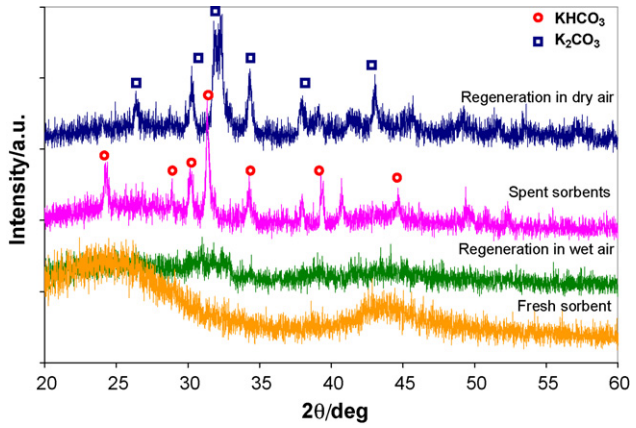

Fig. 14. XRD patterns of K_2CO_3/ACP sorbents under wet and dry regeneration conditions.

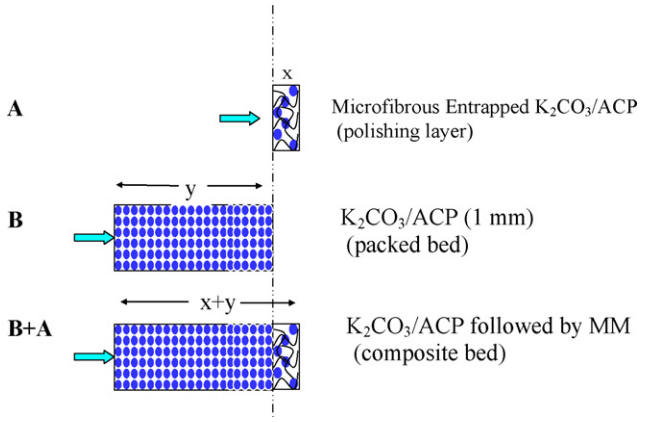

Fig. 15. A schematic of a composite bed design (not to scale).

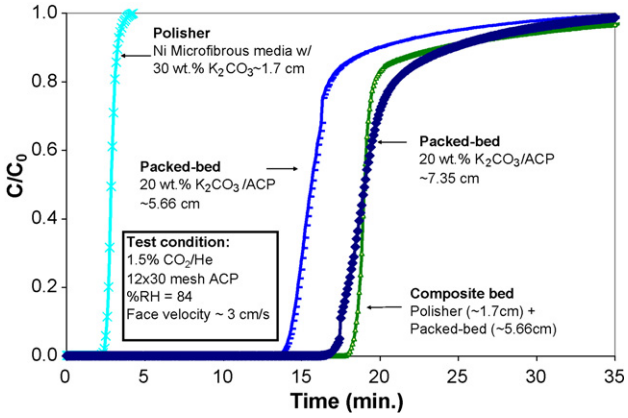

Fig. 16. Comparative BT curves of a composite bed and a packed bed.

steam and dry air. It is shown that regeneration in steam restores 98% carbon dioxide adsorption capacity of the fresh sorbent. However, when the composite sorbent was regenerated in dry air its carbon dioxide adsorption capacity was lost. The regeneration in dry air at 150 °C for 2 h causes the sorbents to lose remaining water in the sorbents and also the crystallization water forming a non-reactive K_2CO_3(s) in the porous matrix. The presence of K_2CO_3 in the composite sorbents after regeneration in dry air is indicated in XRD patterns in Fig. 14. This reaction product, K_2CO_3 is inactive compared to the initial potassium carbonate. The additional water can be added from the gas stream to form a water layer, but hydration reaction is kinetically slow at room temperature. As a result, the water is necessary during regeneration to maintain the water layer and prevent dehydration of K_2CO_3.

The XRD patterns of the fresh composite sorbent and ACP show similar features. This indicates the presence of K_2CO_3(aq) in the porous matrix of ACP. Adsorption of carbon dioxide on the composite sorbents results in the formation of potassium hydrogen carbonate as shown in the presence of $KHCO_3$ peaks on the spent composite sorbent. The spent sorbents were then regenerated in dry and wet air. The sample regenerated in steam shows similar feature as a fresh sorbent indicative of the decomposition of $KHCO_3$ and the formation of K_2CO_3(aq). The composite sorbent regenerated in dry air shows presence of an inactive K_2CO_3(s).

3.5. Composite bed

A composite bed consisting of packed bed of K_2CO_3/ACP sorbents (1 mm pellet) followed by microfibrous entrapped K_2CO_3/ACP polisher was tested. Fig. 15 shows the schematic diagram of a series of breakthrough tests for carbon dioxide adsorption of microfibrous media, packed bed of K_2CO_3 impregnated ACP (1 mm pellet), and composite bed. Microfibrous media with thickness of 1.7 cm (x) and the packed bed of ACP composite sorbents with bed thickness of 5.6 cm (y) are tested for carbon dioxide adsorption capacity. The breakthrough curves are shown in Fig. 16. Fig. 16 shows the comparison of the composite bed and a packed bed of the ACP composite sorbents. It is shown that the composite bed offers higher breakthrough capacity compared to that of the packed bed. However, the improvement from microfibrous media was not pronounced due to the nano-dispersed nature of the packed bed of the prepared composite sorbents as shown in the calculated data in Table 3.

It was found that a composite bed offers higher carbon dioxide adsorption capacity than that of the packed bed at the same volume. Moreover, the breakthrough curve of the

Table 3
Adsorption characteristics of composite sorbents

	Mass (g)	Volume (cm^3)	CO_2 adsorption capacity (g CO_2/total g sorbent)		Adsorption rate constant (min^{-1})
			Breakthrough	Saturation	
Packed bed	7.232	12.99	0.0175	0.0202	1.9165
Composite bed	7.093	13.00	0.0233	0.0254	5.2188

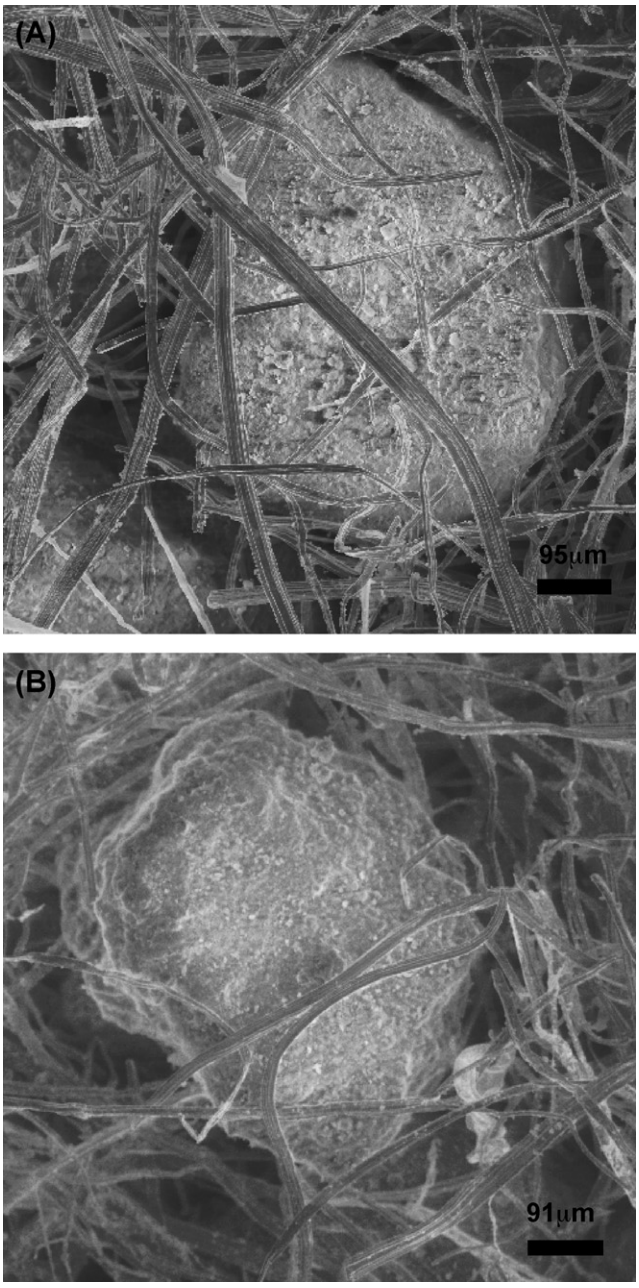

Fig. 17. SEM micrographs of microfibrous media; (A) fresh polisher; (B) spent polisher after eight cycles of regeneration.

composite bed is sharper than that of packed bed indicative of higher sorbent utilization with 63% higher adsorption rate constant.

SEM micrographs in Fig. 17 show the microstructure of the fresh microfibrous entrapped K_2CO_3/ACP sorbents and microfibrous media after eight regeneration cycles. No significant structural changes were observed in the sinter-locked network of the microfibrous media indicative of its robustness and high structural integrity.

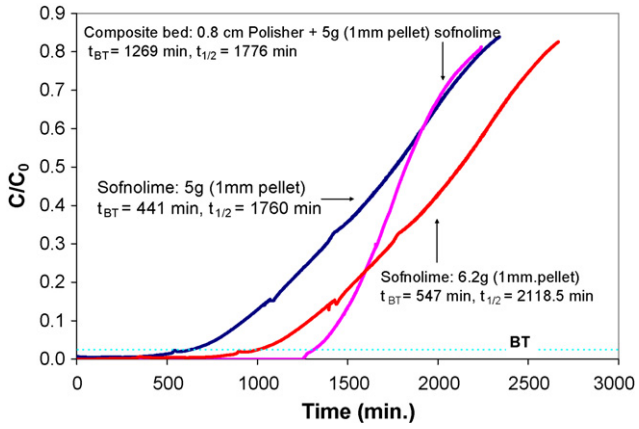

Fig. 18. BT curves of composite bed using Sodalime®.

3.6. Applications of polisher on sodalime

Sodalime is one of the commercially available solid sorbents for CO_2 adsorption. The main application is for use as a packed bed in a scrubber built into ventilation systems for cleaning closed-circuit breathing systems for military and medical applications. The sorbents are $Ca(OH)_2$-based sorbents obtained from Molecular Products (UK). This type of sorbent is often used in submarines. The concept of the composite bed was applied by using a polishing sorbent (∼0.5 g/0.5 cm) backing up five grams of Sodalime. The breakthrough tests were conducted and the results are shown in Fig. 18.

From the breakthrough data, it was found that the composite bed shows higher carbon dioxide adsorption capacity and sharper breakthrough curve compared to that of the packed bed. The carbon dioxide adsorption capacity and adsorption rate constant were then calculated as shown in Table 4. It is shown that the composite bed yields 120% higher breakthrough capacity with 90% higher adsorption rate constant than that of the packed bed of the Sodalime alone. These results indicate the advantages of using microfibrous media in a composite bed. At the same volume, the composite bed offers a sharper breakthrough curve than that of the packed bed indicating that microfibrous media improves sorbent utilization of the packed bed by reducing the critical bed depth allowing the adsorber size and volume to be reduced.

Table 4
Characteristics of Sofnolime in a composite bed design

	Mass (g)	Volume (cm^3)	CO_2 adsorption capacity (g CO_2/total g sorbent)		Adsorption rate constant (min^{-1})
			Breakthrough	Saturation	
Packed bed	6.2	7.38	0.091	0.624	0.0033
Composite bed	5.5	7.84	0.240	0.646	4.4614

4. Conclusions

A regenerable microfibrous entrapped K_2CO_3/ACP sorbents has been developed and evaluated for CO_2 adsorption applications at room temperature. The use of microfibrous media in a composite bed combines the advantage of high volume loading of active sorbents from packed beds and the overall contacting efficiency of small particulates while minimizing the internal mass transfer resistance from a stand alone packed bed. The microfibrous media showed its ability to recover up to 86% CO_2 adsorption capacity after eight regeneration cycles. The advantage of a low temperature reversible liquid phase absorption in an "apparent solid matrix" is as follows:

- High log contacting efficiency in a thin, low pressure drop media.
- Low thermal effects (low regeneration temperature and δH of reaction).
- Capability to use microfibrous media alone or in a composite bed to obtain maximum capacity per unit volume.
- Opportunity to use this approach on low concentration and more sensitive applications (i.e. metal-air batteries).

References

[1] P. Friedlingstein, S. Solomon, Proc. Natl. Acad. Sci. USA 102 (2005) 10832–10836.
[2] X. Xu, C. Song, B. Miller, A.W. Scaroni, Fuel Process. Technol. 86 (2005) 1457–1472.
[3] Z. Yong, V.G. Mata, A.E. Rodrigues, Adsorption 7 (2001) 41–50.
[4] P. Luby, Petroleum Coal 46 (2004) 1–16.
[5] B. Wang, H. Jin, D. Zheng, Int. J. Energy Res. 28 (2004) 521–535.
[6] J.P.H. Fee, J.M. Murray, S.R. Luney, Anaesthesia (Anaesthesia) 50 (1995) 841–845.
[7] B.J. Tatarchuk, US Patent 5,096,663 (1992).
[8] R.A. Overbeek, A.M. Khonsari, Y.F. Chang, L.L. Murrell, B.J. Tatarchuk, M.W. Meffert, US Patent 6,231,792 (2001).
[9] B.J. Tatarchuk, US Patent 5,102,745 (1992).
[10] D.K. Harris, D.R. Cahela, B.J. Tatarchuk, Compos. Part A 32 (2001) 1117–1126.
[11] Y. Yoon, J. Nelson, Am. Ind. Hyg. Assoc. J. 48 (1984) 509–516.
[12] A. Roine, HSC Chemistry for Windows, Version 4.0, Outokumpu Research Oy, Pori, Finland, 1999.